Since January 2020 Elsevier has created a COVID-19 resource centre with free information in English and Mandarin on the novel coronavirus COVID-19. The COVID-19 resource centre is hosted on Elsevier Connect, the company's public news and information website.

Interferon antagonism by SARS-CoV-2: a functional study using reverse genetics

Simon Schroeder, Fabian Pott, Daniela Niemeyer, Talitha Veith, Anja Richter, Doreen Muth, Christine Goffinet, Marcel A Müller, Christian Drosten**

Summary

Background The COVID-19 agent, SARS-CoV-2, is conspecific with SARS-CoV, the causal agent of the severe acute respiratory syndrome epidemic in 2002–03. Although the viruses share a completely homologous repertoire of proteins and use the same cellular entry receptor, their transmission efficiencies and pathogenetic traits differ. We aimed to compare interferon antagonism by SARS-CoV and SARS-CoV-2.

Methods For this functional study, we infected Vero E6 and Calu-3 cells with strains of SARS-CoV and SARS-CoV-2. We studied differences in cell line-specific replication (Vero E6 *vs* Calu-3 cells) and analysed these differences in relation to TMPRSS2-dependent cell entry based on inhibition with the drug camostat mesilate. We evaluated viral sensitivity towards type I interferon treatment and assessed cytokine induction and type I interferon signalling in the host cells by RT-PCR and analysis of transcription factor activation and nuclear translocation. Based on reverse genetic engineering of SARS-CoV, we investigated the contribution of open reading frame 6 (ORF6) to the observed phenotypic differences in interferon signalling, because ORF6 encodes an interferon signalling antagonist. We did a luciferase-based interferon-stimulated response element promotor activation assay to evaluate the antagonistic capacity of SARS-CoV-2 wild-type ORF6 constructs and three mutants (Gln51Glu, Gln56Glu, or both) that represent amino acid substitutions between SARS-CoV and SARS-CoV-2 protein 6 in the carboxy-terminal domain.

Findings Overall, replication was higher for SARS-CoV in Vero E6 cells and for SARS-CoV-2 in Calu-3 cells. SARS-CoV-2 was reliant on TMPRSS2, found only in Calu-3 cells, for more efficient entry. SARS-CoV-2 was more sensitive to interferon treatment, less efficient in suppressing cytokine induction via IRF3 nuclear translocation, and permissive of a higher level of induction of interferon-stimulated genes *MX1* and *ISG56*. SARS-CoV-2 ORF6 expressed in the context of a fully replicating SARS-CoV backbone suppressed *MX1* gene induction, but this suppression was less efficient than that by SARS-CoV ORF6. Mutagenesis showed that charged amino acids in residues 51 and 56 shift the phenotype towards more efficient interferon antagonism, as seen in SARS-CoV.

Interpretation SARS-CoV-2 ORF6 interferes less efficiently with human interferon induction and interferon signalling than SARS-CoV ORF6. Because of the homology of the genes, onward selection for fitness could involve functional optimisation of interferon antagonism. Charged amino acids at positions 51 and 56 in ORF6 should be monitored for potential adaptive changes.

Funding Bundesministerium für Bildung und Forschung, EU RECOVER project.

Lancet Microbe 2021; 2: e210–18

Published Online March 4, 2021 https://doi.org/10.1016/S2666-5247(21)00027-6

*Joint study supervisors

Institute of Virology, Charité-Universitätsmedizin Berlin, Berlin, Germany (S Schroeder MSc, F Pott MSc, D Niemeyer PhD, T Veith MPhil, A Richter, D Muth PhD, Prof C Goffinet PhD, M A Müller PhD, Prof C Drosten PhD); **Berlin Institute of Health, Berlin, Germany** (F Pott, Prof C Goffinet, Prof C Drosten); **Deutsches Zentrum für Infektionsforschung, Associated Partner Charité-Universitätsmedizin Berlin, Berlin, Germany** (D Muth, Prof C Drosten); **Martsinovsky Institute of Medical Parasitology, Tropical and Vector Borne Diseases, Sechenov University, Moscow, Russia** (M A Müller)

Correspondence to: Prof Christian Drosten, Institute of Virology, Charité-Universitätsmedizin, Berlin 10117, Germany **christian.drosten@charite.de**

Introduction

Since its identification as the causal agent of a novel viral pneumonia in late 2019, SARS-CoV-2 has rapidly shifted from causing initial local case clusters of COVID-19 in the Hubei province of China to a pandemic.[1] The novel virus is the same species as SARS-CoV, the causal agent of the severe acute respiratory syndrome epidemic in 2002–03.[2] SARS-CoV-2 and SARS-CoV share striking similarities in their genomic architecture as well as receptor and host protease usage.[3,4] However, SARS-CoV-2 is distinct from SARS-CoV in its clinical and epidemiological presentation, with lower pathogenicity and case-fatality rate but higher human-to-human transmission rate and incidence.[5]

Pathogenicity and transmissibility are often a function of host cell entry capacity and tropism. Clinical observations suggest that SARS-CoV-2 replicates in the upper and lower respiratory tract, whereas SARS-CoV mainly replicates in the lower respiratory tract, despite identical receptor usage.[6] This altered tropism might be a function of cofactor distribution, such as the distribution of host membrane proteases,[4,7] or of increased binding capacity to the host receptor, ACE2.[8]

Another factor in virus pathogenicity and transmissibility is the evasion of innate immunity. Type I interferons are among the first cytokines to be upregulated in virus-infected cells and are important in coordinating the antiviral response and inflammation. Interferon signalling triggers the expression of more than 300 antiviral proteins and chemokines, inducing an antiviral state in host cells.[9] Resilience towards interferon-mediated innate immunity

Research in context

Evidence before this study

We searched PubMed for studies published in English from database inception to Aug 18, 2020, on the interaction between SARS-CoV-2 and the innate immune response. We used the search terms "severe acute respiratory syndrome coronavirus 2", "SARS-CoV-2", "novel coronavirus", "2019-nCoV", or "COVID-19"; and "interferon", "innate immunity", "host response", "protein 6", "reverse genetics", or "antagonism". We found seven studies that looked at interferon induction or cytokine induction in laboratory infections of lung tissue, lung-derived cells, gut organoids, or patient bronchoalveolar fluid material. Results on cytokine induction differed between these studies, depending on the applied system. Interferon-sensitive gene induction was studied in four of these studies, with partially different results. One study looked at interferon sensitivity based on cell culture and found SARS-CoV-2 to be more sensitive against interferon treatment than SARS-CoV. All studies were based mainly on gene expression analysis. We found three studies that did ORF6 overexpression-based interferon stimulation response element promotor activation assays, all indicating a role of open reading frame 6 (ORF6) in interferon signalling antagonism. One additional study published during revision of the present study found an interaction between ORF6 and nuclear pore protein Nup98 that is compatible with our observations, but the study did not compare SARS-CoV and SARS-CoV-2 interferon antagonism phenotypes. To our knowledge, no reverse genetic studies on the anti-interferon activity of individual SARS-CoV-2 genes have been published.

Added value of this study

We show that SARS-CoV-2 is less efficient in evading the host innate immune response and more sensitive to interferon treatment than SARS-CoV. Earlier studies of ORF6 function were based on protein overexpression, which makes it difficult to draw quantitative conclusions. The present study identifies quantitative phenotypic differences by gene exchange in the context of an otherwise constant, replicating viral genome. It also adds novel information regarding the function of ORF6. Whereas a conserved residue (amino acid Met58) was previously found to be essential for Nup98 interaction in both viruses, the present study describes an additional variable trait via positions 51 and 56 linked to the intensity of interferon antagonism by both viruses.

Implications of all the available evidence

Because the genes that encode protein 6 in SARS-CoV and SARS-CoV-2 are homologous, there might be room for functional optimisation during onward evolution of SARS-CoV-2 in humans. Ongoing molecular surveillance should focus on changes in ORF6 that could indicate an increase of interferon antagonism and virulence, including changes in positions 51 and 56.

is a hallmark of virulence and pathogenicity in coronaviruses and many other viruses. Coronaviruses counteract the antiviral effects of interferons and are sensitive to therapeutic application of interferons if administered early.[10,11]

It is unclear whether differences in receptor usage determine all the differences in disease presentation between SARS-CoV and SARS-CoV-2. Differences in interferon system evasion and antagonism might also play an important role. First studies of genes in SARS-CoV-2 that might encode for interferon antagonists based on their homology to SARS-CoV have been done. Among all previously described SARS-CoV interferon antagonists (nsp1, nsp3, nsp14, nsp15, nsp16, protein 6, protein 8, N), protein 6 shows the highest amino acid sequence divergence between SARS-CoV and SARS-CoV-2.[12] In both SARS-CoV and SARS-CoV-2, protein 6 has been shown to prevent interferon-stimulated gene induction by interacting with importin subunits α-1 and β-1 (KPNA1 and KPNB1), which are required for STAT1 nuclear translocation and interferon-stimulated gene induction.[13,14] Furthermore, SARS-CoV-2 protein 6 interferes with STAT1 translocation by binding to Nup93, a key component of nuclear pore complexes.[14] Other overexpression studies describe an antagonistic function of SARS-CoV-2 protein 6 in the interferon-stimulated response element (ISRE) and interferon promotor activation assays.[15,16] However, because previous studies have relied on ectopic protein overexpression, understanding the relevance and quantitative contribution of genotype differences to phenotype remains difficult. Therefore, we aimed to compare interferon evasion phenotypes of SARS-CoV and SARS-CoV-2 using live virus isolates and mutagenesis studies in the context of a full viral genome by reverse genetics.

Methods

Study design, cell cultures, and virus isolates

The experimental study design comprised infection of permanent cell lines with and without ruxolitinib, interferon beta, or camostat mesilate. We used Calu-3 cells (American Type Culture Collection [ATCC] HTB-55), Vero E6 cells (ATCC CRL-1586), as well as Vero-TMPRSS2 cells (donated by Stefan Pöhlmann and Markus Hoffmann, German Primate Center, Göttingen, Germany).[4] We used SARS-CoV-2 strain Munich/2020/984 (BetaCoV/Munich/BavPat1/2020; EPI_ISL_406862),[5] SARS-CoV-2 strain Victoria (BetaCoV/Australia/VIC01/2020; GenBank accession number MT007544), and SARS-CoV strain Frankfurt (GenBank accession number AY310120). The use of stored clinical samples without person-related data is covered by section 25 of the Berlin hospital law and does not require ethical or legal clearance. The ethical committee has been

notified of the study and acknowledged receipt under file number EA1/369/20.

Procedures and outcomes

For all experimental procedures, the detailed methods are provided in appendix 1 (pp 2–6). Sequences of oligonucleotides are also provided in appendix 1 (p 14).

To evaluate the replication of SARS-CoV and SARS-CoV-2 (Munich strain), we infected Vero E6 and Calu-3 cells at low multiplicity of infection (MOI) of 0·001. To determine the effect of blunting the type I interferon response on virus replication in Calu-3 cells, we pretreated the cells for 2 h with 100 nM ruxolitinib (Invivogen, San Diego, CA, USA), a Janus kinase inhibitor. Double-stranded RNA (dsRNA) replication intermediates were measured at 16 h post infection by immunofluorescent analysis. Infectious particle production was determined by plaque titration at 24 h post infection. Interferon beta treatment (Biochrom, Berlin, Germany; added 1 h before infection at 10, 100, 400, 1000, and 2000 international units [IU] per mL and 1 h post infection at 100, 400, 1000, 2000, and 4000 IU/mL) was assessed in Vero E6 and Calu-3 cells. We used higher concentrations of interferon beta for post-infection treatment because we expected a smaller effect compared with interferon beta treatment before infection. We quantified virus replication by plaque titration at 24 h post infection. To assess the effect of interferon treatment on the replication cells infected with SARS-CoV and SARS-CoV-2, we normalised infectious virus progeny of cell cultures treated with interferon beta against the progeny obtained from untreated cultures by setting untreated samples to 100%. Further information on the treatments with interferon beta and ruxolitinib is provided in appendix 1 (pp 2–3).

Because coronaviruses might actively antagonise expression of antiviral cytokines,[13,17–19] we evaluated cytokine expression in single-cycle infections, infecting Calu-3 cells at MOI of 1. We included two strains of SARS-CoV-2 (Munich and Victoria) to investigate any strain-specific differences. We quantified the mRNA induction of *IFNB1*, *IFNL1*, *CCL5*, *MX1*, and *ISG56* in infected Calu-3 cells at 12 h, 16 h, and 24 h post infection by quantitative RT-PCR. We calculated the fold inductions relative to non-infected control cells, normalised to the housekeeping gene *TBP* using the ΔΔCt method for each experiment. We assessed IRF3 nuclear translocation in Calu-3 cells infected at MOI of 1 by confocal microscopy at 16 h and 24 h post infection and quantified the nuclear and cytosolic IRF3 signal intensities. To further characterise the interference with interferon induction, we tested downstream activation of essential signalling pathways by western blot analysis. We infected Calu-3 cells with viruses at MOI of 0·5, followed by western blot analysis. We probed cellular lysates with antibodies against the following proteins: IRF3, phospho-IRF3, IκBα, cross-reactive SARS-CoV N, and β-actin (loading control). We analysed nuclear translocation of STAT1 and NF-κB upon infection by nuclear-cytosolic fractionation and western blot analysis using antibodies against STAT1, NF-κB, GAPDH (cytosolic fraction control), histone H3 (nuclear fraction control), and β-actin (loading control).

See Online for appendix 1

SARS-CoV-2 has been shown to make more efficient use of spike protein priming by the transmembrane protease TMPRSS2 than SARS-CoV.[4] Because Calu-3 cells, but not Vero cells, express TMPRSS2,[20,21] we studied the contribution of TMPRSS2 to replication of both viruses using Vero cells transgenic for *TMPRSS2*. We used original clinical samples from five different patients with acute SARS-CoV-2 infection to avoid any previous viral adaptation to Vero cells. Virus progeny was quantified by RT-PCR at 72 h post infection, which is our standard timepoint for readout when infecting cells with clinical samples for routine virus isolation. We also assessed the effect of chemical inhibition of TMRPSS2 on virus replication by camostat mesilate treatment (100 nM camostat mesilate before infection at MOI of 0·01) by titration of virus progeny and immunofluorescent microscopy, in which we evaluated cytosolic dsRNA staining intensity using ImageJ version 1.53 (National Institutes of Health, Bethesda, MD, USA; appendix 1 pp 2–5).

To study the antagonistic function of SARS-CoV-2 protein 6 against JAK-STAT-dependent interferon signal transduction,[13–16] we constructed recombinant SARS-CoV mutants in which we replaced SARS-CoV open reading frame 6 (ORF6) with SARS-CoV-2 ORF6 (rSARS-CoV$_{ORF6\text{-}SARS\text{-}2}$), as well as an ORF6 knockout mutant (rSARS-CoV$_{\Delta ORF6}$), in which the fourth and fifth codon of ORF6 were replaced with stop codons. We evaluated the replication of wild-type and mutant rSARS-CoV in Calu-3 and Vero E6 cells. We infected both cell lines at MOI of 0·001 and quantified virus replication at 48 h post infection by plaque titration. To evaluate differences in interferon induction, we infected Calu-3 cells at MOI of 1 with wild-type and mutant rSARS-CoV and quantified the mRNA induction of *IFNB1*, *IFNL1*, and *CCL5* at 16 h post infection. We also quantified viral genomic RNA (genome equivalents per mL) and subgenomic mRNA 6 in Calu-3 cells and normalised these to *TBP* mRNA levels.

To evaluate the antagonistic function of SARS-CoV-2 protein 6 in interferon signalling, we did single-cycle infection experiments (MOI of 1) in Vero E6 cells. We allowed for 16 h of infection and viral protein expression before exposure of cells to 0 IU/mL, 250 IU/mL, or 500 IU/mL pan-species type I interferon for 30 min to cause JAK-STAT-mediated induction of interferon-stimulated genes. We quantified the mRNA induction of the interferon-stimulated genes *MX1* and *ISG56* 8 h post treatment relative to non-infected control cells. We also quantified viral genomic RNA and normalised this to *TBP* mRNA level.

We investigated whether differential amino acid composition of SARS-CoV and SARS-CoV-2 protein 6 could explain the reduced antagonist capacity of SARS-CoV-2 protein 6. We focused on differences in charged amino acid composition in the carboxy-terminal domain (CTD) of protein 6, because these residues were previously shown to drive the antagonistic function of SARS-CoV protein 6.[13] We identified two residues in the CTD (Gln51 and Gln56) that show a loss-of-charge substitution in SARS-CoV-2 compared with SARS-CoV (Glu51 and Glu56). We constructed SARS-CoV-2 overexpression plasmids encoding wild-type protein 6 (Gln51, Gln56) as well as constructs with substitutions Gln51Glu, Gln56Glu, or both. We did a luciferase-based ISRE promotor assay with these ORF6 constructs. We measured the luciferase activity 18 h post interferon treatment (200 IU/mL pan-species interferon) in HEK-293T cells transfected with 50 ng ORF6 and control constructs (50 ng Nipah virus V protein, a known interferon antagonist) and calculated the luciferase activity in each sample by normalisation to cells transfected with empty vector. We confirmed expression of each construct by western blot analysis of lysed HEK-293T cells.

To obtain an overview of the frequency of changes at positions 51 and 56 in circulating viruses, we screened all 65 069 SARS-CoV-2 sequences available on GISAID (as of Aug 12, 2020).

For **GISAID** see https://www.gisaid.org/

Statistical analysis

Experiments and replications were designed according to prespecified hypotheses based on pilot experiments and experience with similar experimental approaches. Information on replicates, parameters, and other details of the experiments is provided in appendix 2. We applied the Shapiro-Wilk normality test on all datasets to confirm normal distributions. Unpaired, two-tailed Student's *t* tests were then used for comparisons of groups. Groups were defined as treated versus untreated samples, SARS-CoV-infected samples versus SARS-CoV-2-infected samples, and samples transfected with different plasmid constructs. All tests were done in GraphPad Prism (version 8.2.1; GraphPad, San Diego, CA, USA). p values of less than 0·05 were considered to be statistically significant. In the experiment comparing replication of SARS-CoV and SARS-CoV-2 in cells treated with interferon beta, replication was normalised to untreated samples to allow for direct comparison of the effect of interferon treatment on replication, regardless of the replication phenotypes in Calu-3 or Vero E6 cells. We calculated the means and SDs for the interferon-treated samples of the four experimental replicates after normalisation and expressed these as a percentage of untreated replication.

See **Online** for appendix 2

Role of the funding source

The funders of the study had no role in study design, data collection, data analysis, data interpretation, or writing of the report.

Results

For this functional study, we infected Vero E6 and Calu-3 cells with strains of SARS-CoV and SARS-CoV-2. In Vero E6 cells, which lack type I interferon genes,[22] SARS-CoV grew to 36-times higher titres than SARS-CoV-2 at 24 h after inoculation with MOI of 0·001. In Calu-3 cells, which are considered largely functional in interferon induction and response,[23] SARS-CoV-2 infection yielded five-times higher titres at 24 h compared with SARS-CoV (figure 1A). In terms of viral growth, SARS-CoV induced a stronger cytopathic effect in Vero cells and SARS-CoV-2 induced a stronger cytopathic effect in Calu-3 cells (appendix 1 p 7).

In Calu-3 cells, treatment with the JAK inhibitor ruxolitinib enhanced infection by both viruses, as assessed by quantification of dsRNA replication intermediates and infectious particle production, suggesting that both viruses are sensitive to a naturally induced interferon-mediated antiviral response (figure 1B–E).

SARS-CoV-2 was more sensitive to interferon pretreatment than SARS-CoV, particularly in Vero E6 cells (figure 2, appendix 1 p 8). 1000 IU/mL interferon beta reduced mean SARS-CoV-2 replication to 1·31% (SD 1·01) of replication levels in untreated Vero E6 cells, whereas SARS-CoV replication was unchanged (figure 2B). In Calu-3 cells, pretreatment with 1000 IU/mL interferon beta reduced mean SARS-CoV-2 replication to 0·68% (0·11) and SARS-CoV replication to 6·02% (4·14) of replication levels in untreated control cells (figure 2A).

Compared with interferon beta pretreatment, differences in viral replication were generally less pronounced with interferon beta applied 1 h after infection. In Calu-3 cells, treatment with 1000 IU/mL interferon beta 1 h after infection reduced mean SARS-CoV-2 replication to 58·26% (SD 13·39) and SARS-CoV replication to 17·08% (5·61) of the level in untreated cells (figure 2C). In Vero E6 cells, mean SARS-CoV-2 replication was reduced to 11·24% (8·49) and SARS-CoV replication to 81·42% (52·74; figure 2D).

Induction of the IRF3-regulated genes *IFNB1* and *IFNL1*, as well as of the IRF3-regulated and NF-κB-regulated gene *CCL5* was significantly higher after SARS-CoV-2 infection compared with SARS-CoV infection of Calu-3 cells (figure 3A). This finding indicates a less efficient counteraction of infection-triggered cytokine induction by SARS-CoV-2.

IRF3, an activator of interferon gene transcription, was retained in the cytoplasm of SARS-CoV-infected cells (figure 3B–E).[24,25] By contrast, after SARS-CoV-2 infection, IRF3 readily translocated into the nucleus, suggesting that the mechanism of SARS-CoV-mediated retention of IRF3 is not conserved in SARS-CoV-2. In accordance with efficient IRF3 translocation, we detected phosphorylated IRF3 in lysates of SARS-CoV-2-infected Calu-3 cells but not SARS-CoV-infected or mock-infected Calu-3 cells (figure 3F, appendix 1 p 15). Lower levels of the NF-κB inhibitor, IκBα, were

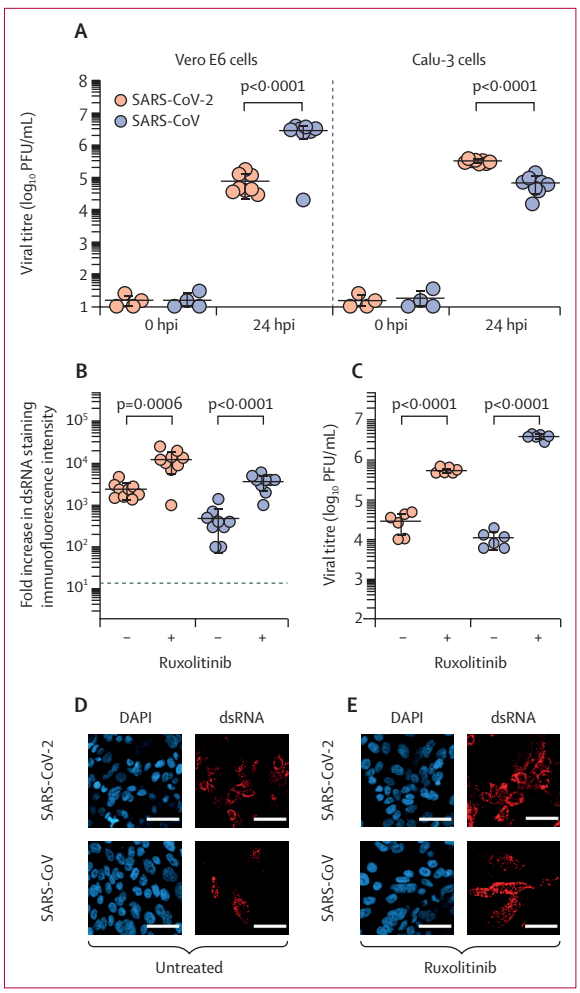

Figure 1: **Replication of SARS-CoV-2 and SARS-CoV in Vero E6 and Calu3 cells and effect of ruxolitinib treatment**

(A) Viral replication in multicycle infections (MOI=0·001) in Vero E6 and Calu-3 cells. Virus replication with or without treatment with 100 nM ruxolitinib in Calu-3 cells (MOI=0·001): measured by immunofluorescence intensity of dsRNA staining at 16 hpi, quantified as fold increase compared with uninfected cells (B); measured by plaque titrations at 24 hpi (C); or qualitatively observed by immunofluorescence microscopy (D, E). In A–C, bars indicate means and SDs (numeric values shown in appendix 1 pp 16–22). In D and E, representative images of dsRNA staining in cells are shown (DAPI [nucleus] staining is shown in blue and dsRNA antibody is shown in red). The scale bar represents 50 μM. dsRNA=double-stranded RNA. hpi=hours post infection. MOI=multiplicity of infection. PFU=plaque-forming unit.

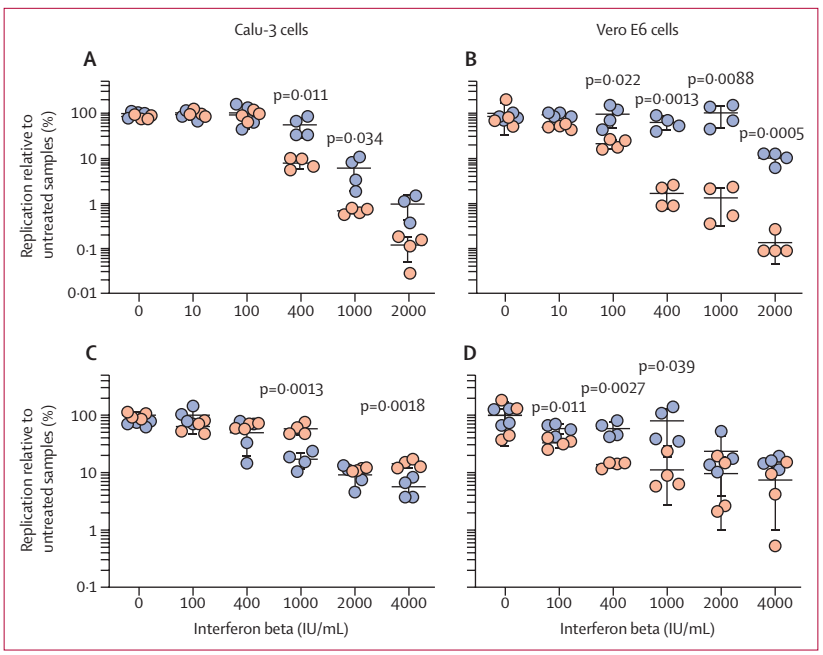

Figure 2: **Replication of SARS-CoV and SARS-CoV-2 in Vero E6 and Calu-3 cells treated with interferon beta before and after infection**

(A, B) Cells pretreated with interferon beta 18 h before infection. (C, D) Cells treated 1 hpi. Virus replication was quantified by plaque titration at 24 hpi and expressed as a percentage of replication (in PFU/mL) in untreated samples; non-normalised data in PFU/mL are presented in appendix 1 (p 8). Bars indicate means and SDs (numeric values shown in appendix 1 pp 16–22). hpi=hours post infection. PFU=plaque-forming units.

detectable in lysates of SARS-CoV-2-infected cells, which is consistent with increased *CCL5* mRNA induction. Probing NF-κB in nuclear and cytosolic cell fractions showed more efficient NF-κB nuclear translocation in cells infected with SARS-CoV-2 than those infected with SARS-CoV (figure 3G, appendix 1 p 15). STAT1 was more efficiently translocated to the nucleus after infection with SARS-CoV-2 than with SARS-CoV (figure 3G, appendix 1 p 15). Consistent with this result, the interferon-stimulated genes *MX1* and *ISG56* were induced more efficiently after infection with SARS-CoV-2 than with SARS-CoV (figure 3H).

SARS-CoV-2 consistently replicated to more than ten-times higher levels in Vero-TMPRSS2 cells compared with Vero E6 cells (appendix 1 p 9). Application of the TMPRSS2 inhibitor camostat mesilate to Calu-3 cells resulted in a more pronounced reduction of infection rate (based on number of cells showing dsRNA staining) and replication level (based on virus titre) for SARS-CoV-2 than for SARS-CoV (appendix 1 p 9).

Recombinant SARS-CoV mutants in which we replaced SARS-CoV ORF6 with the full-length ORF6 of SARS-CoV-2 (rSARS-CoV$_{ORF6\text{-}SARS\text{-}2}$) or deleted ORF6 by replacing the fourth and fifth codon of ORF6 with stop codons (rSARS-CoV$_{\Delta ORF6}$; appendix 1 p 10) were replication-competent and showed the same level of expression of ORF6-specific subgenomic RNA (appendix 1 p 16). In multicycle infections in interferon-competent Calu-3 cells (MOI=0·001), both rSARS-CoV$_{ORF6\text{-}SARS\text{-}2}$ and rSARS-CoV$_{\Delta ORF6}$ replicated more than ten-times less efficiently than wild-type rSARS-CoV, whereas replication levels were similar in interferon-deficient Vero E6 cells (figure 4A and 4B), as well as in Calu-3 cells under single-cycle infection conditions (MOI=1; figure 4C). There was no significant difference in mRNA induction of *IFNB1*, *IFNL1*, and *CCL5* (figure 4D–F).

Induction of the interferon-stimulated gene *MX1*, the induction of which is strictly dependent on interferon signaling,[26] was quantified after 8 h (figure 4H). Whereas rSARS-CoV$_{ORF6\text{-}SARS\text{-}2}$ suppressed *MX1* induction to a lesser

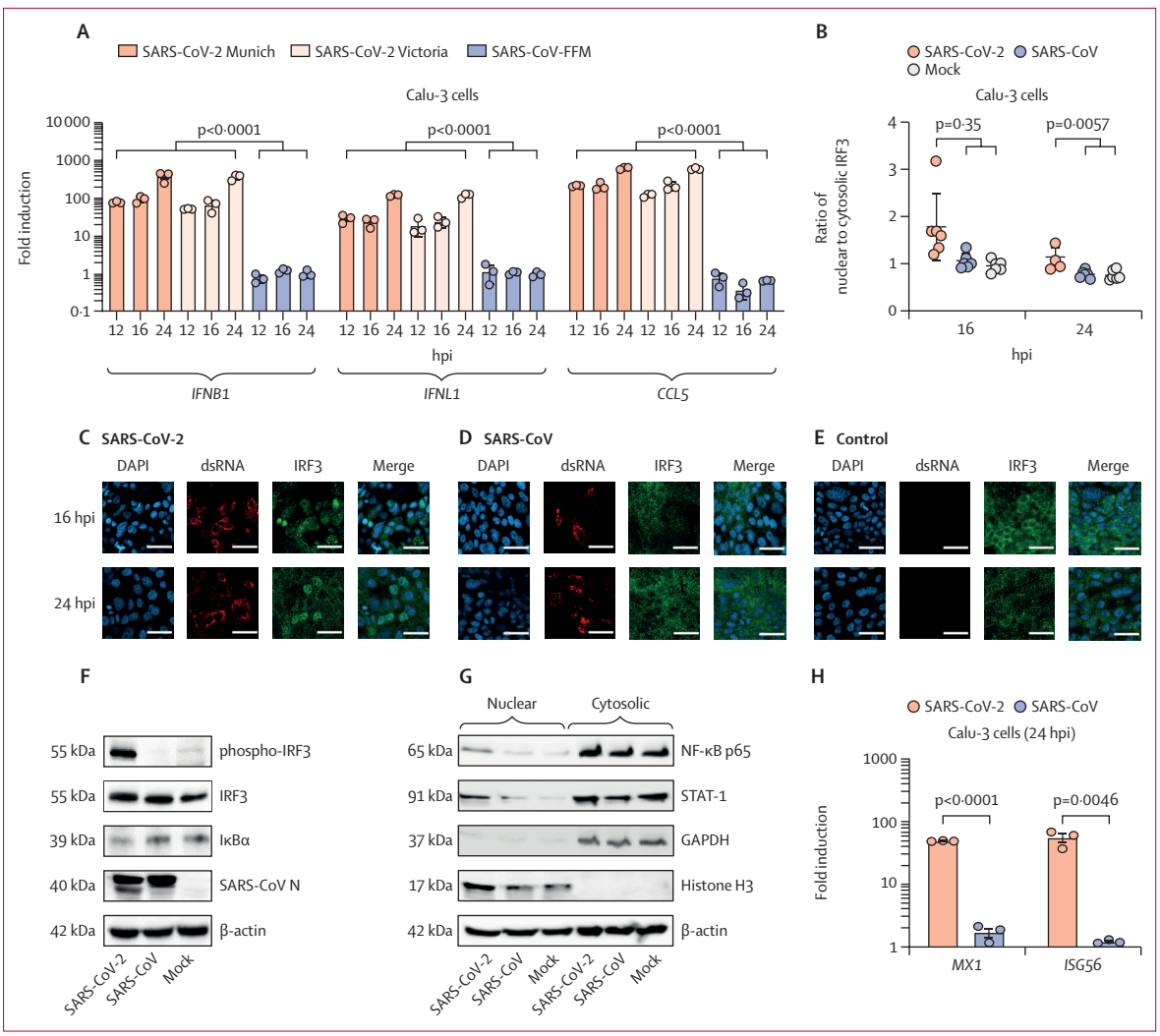

Figure 3: **Interferon and cytokine induction in Calu-3 cells infected with SARS-CoV and SARS-CoV-2**
(A) Quantitative RT-PCR analysis of cytokine mRNA induction in Calu-3 cells (MOI=1) at 12 hpi, 16 hpi, and 24 hpi. (B) Quantification of nuclear and cytosolic IRF3 signal intensities from immunofluorescence imaging (bars indicate means and SDs). (C–E) Representative immunofluorescent images of Calu-3 cells infected with SARS-CoV-2 or SARS-CoV (and non-infected controls), which were fixed and stained for dsRNA and IRF3 at 16 hpi and 24 hpi. DAPI (nucleus) staining is shown in blue, dsRNA antibody is shown in red, IRF3 antibody is shown in green, and the merged images show both DAPI and IRF3 staining. The scale bar represents 50 μM. (F, G) Western blot analyses of lysed Calu-3 cells. Quantification of band intensities is provided in appendix 1 (p 15). (H) Quantitative RT-PCR analysis of *MX1* and *ISG56* mRNA induction in Calu-3 cells infected with SARS-CoV-2 and SARS-CoV (MOI=1) at 24 hpi. Columns and bars show means and SDs (numeric values shown in appendix 1 pp 16–22). dsRNA=double-stranded RNA. hpi=hours post infection. MOI=multiplicity of infection.

degree than the wild-type, induction was strongest in cells infected with rSARS-CoV$_{\Delta ORF6}$, suggesting that a residual antagonistic function is preserved in SARS-CoV-2 ORF6. Of note, we found that the induction phenotype of *ISG56* showed less pronounced differences between rSARS-CoV$_{ORF6\text{-}SARS\text{-}2}$ and rSARS-CoV$_{\Delta ORF6}$ (figure 4I). The induction of *ISG56* is mediated not only by JAK-STAT signalling, but also by IRF3 signalling.[27] Therefore, subtle differences in *ISG56* induction by JAK-STAT signalling alone could be masked by IRF3-mediated *ISG56* induction, which is not impeded by the antagonistic functions of protein 6 (figure 4D–F). No difference in virus load was observed by RT-PCR, excluding the possibility that differences in interferon-stimulated gene induction were caused by differential growth of mutant viruses under the conditions of the experiment (figure 4G).

SARS-CoV-2 ORF6 overexpression constructs expressing CTD charged residues, as found in SARS-CoV ORF6 (Gln51Glu, Gln56Glu, or both; appendix 1 p 11) showed reduced ISRE promotor activation compared with wild-type SARS-CoV-2 ORF6 (figure 4J). This result supports the suggestion that charged amino acids in positions 51 and 56 contribute to the increased interferon antagonistic capacity of SARS-CoV protein 6. SARS-CoV and SARS-CoV-2 wild-type constructs did not differ in this assay, reflecting that phenotypic differences might

not become apparent at the high expression level used in this assay.

We identified two SARS-CoV-2 sequences uploaded to GISAID (as of Aug 12, 2020) that encode substitutions from non-charged to positively charged residues at positions 51 and 56 (Gln51Lys EPI_ISL_487291 [South Africa] and Gln56Arg EPI_ISL_433754 [UK]; appendix 1 pp 12–13). Several individual sequences per mutant were contained in GISAID, and the mutants were spatiotemporally clustered, suggesting that mutants were transmitted. However, we note that the charge with both Gln51Glu and Gln56Glu, as in SARS-CoV, is negative.

Discussion

The results of this study suggest that SARS-CoV-2 suppresses cytokine induction and interferon signalling with lower efficiency than SARS-CoV, despite the shared genome architecture and expression of homologous viral proteins, and that only interferon signalling is linked to protein 6.

Multiple viral proteins are known to facilitate interferon antagonism in SARS-CoV. IRF3, an activator of interferon gene transcription, was found to be retained in the cytoplasm of cells infected with SARS-CoV but not SARS-CoV-2.[24,25] Low IRF3 cytoplasmic retention in cells infected with SARS-CoV-2 might explain the higher induction of the IRF3-regulated genes *IFNB1* and *IFNL1*. A less efficient counteraction of SARS-CoV-2 against interferon induction did not correspond to our initial observation of more efficient growth of SARS-CoV-2 than SARS-CoV in fully interferon-competent Calu-3 cells, and vice versa in Vero E6 cells, confirming observations also made by others.[28] Of note, the general growth advantage of SARS-CoV-2 in Calu-3 cells might be determined by its preferential use of TMPRSS2-dependent entry. SARS-CoV nsp1 and nsp3 prevent IRF3 phosphorylation, which is essential for nuclear translocation, thereby preventing interferon induction.[29–31] Nsp1 prevents STAT1 phosphorylation upon interferon receptor binding.

Although genes encoding intereferon antagonists are highly conserved between SARS-CoV and SARS-CoV-2, the protein 6 gene is less conserved. In cells infected with

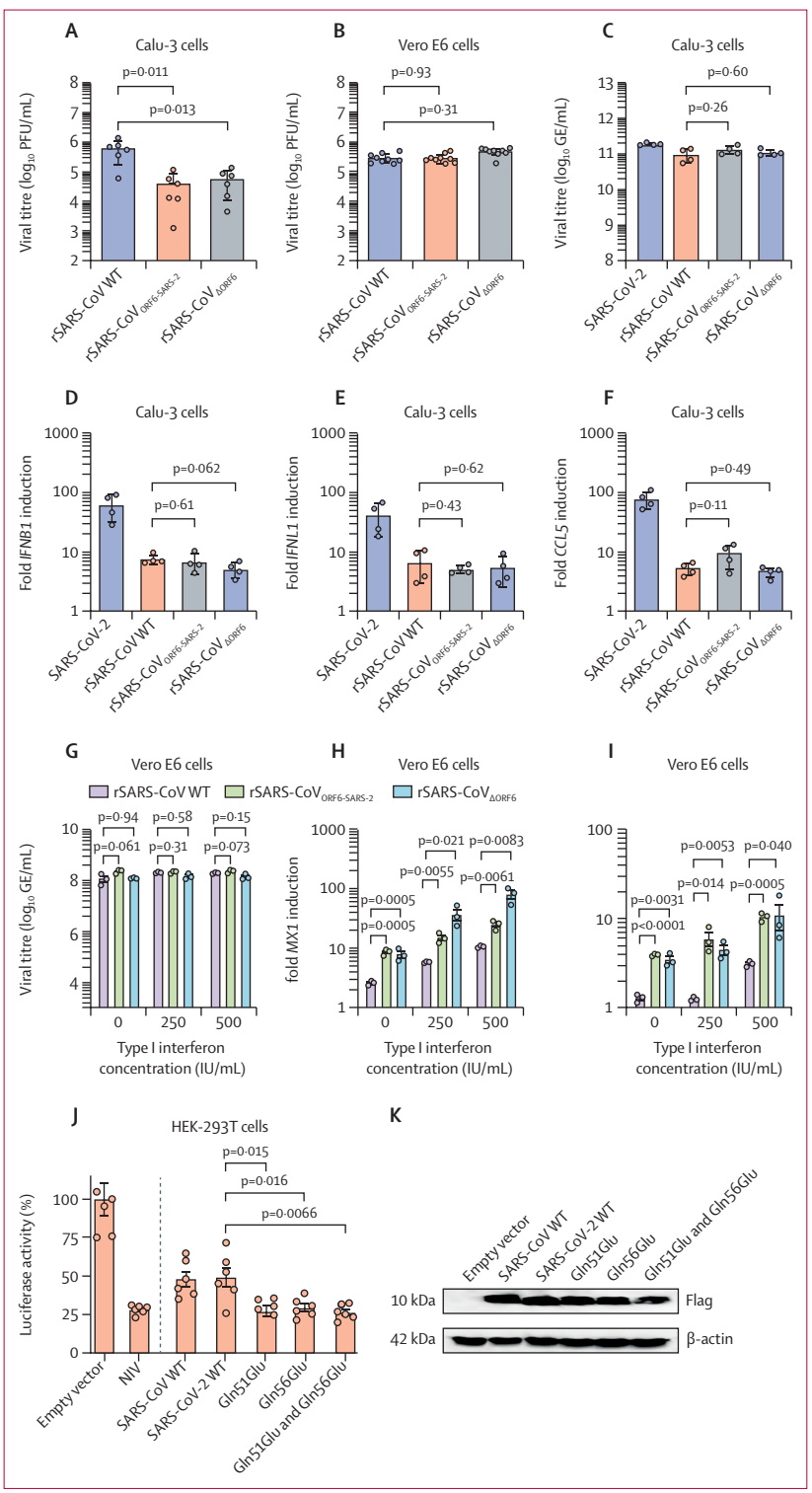

Figure 4: **Functional characterisation of rSARS-CoV ORF6 constructs**
(A, B) Viral replication measured in multicycle infections (MOI=0·001) of all recombinant viruses in Calu-3 and Vero E6 cells at 48 hpi. (C–F) Single cycle infection (MOI=1) of Calu-3 cells with SARS-CoV-2 and recombinant SARS-CoV mutants: (C) intracellular virus load at 16 hpi and (D–F) induction of *IFNB1*, *IFNL1*, and *CCL5* mRNA transcripts at 16 hpi. (G–I) Vero E6 cells infected with recombinant SARS-CoV mutants (MOI=1) treated for 30 min with pan-species type I interferon at 16 hpi: (G) intracellular virus load and (H, I) induction of *MX1* and *ISG56* mRNA transcripts at 24 hpi. (J) Luciferase-based interferon-stimulated response element promotor assay in HEK-293T cells. Luciferase activity (normalised against empty vector samples) was measured at 18 h after 200 IU/mL interferon treatment. Error bars show SD. (K) Protein expression levels of ORF6 constructs, assessed by western blot analysis of lysed HEK-293T cells. Numeric values for means and SDs are shown in appendix 1 (pp 16–22). GE=genome equivalents. hpi=hours post infection. IU=international units. MOI=multiplicity of infection. NiV=Nipah virus V protein. PFU=plaque-forming units. rSARS-CoV WT=wild-type recombinant SARS-CoV. rSARS-CoV$_{ORF6\text{-}SARS\text{-}2}$=recombinant SARS-CoV with SARS-CoV ORF6 replaced by SARS-CoV-2 ORF6. rSARS-CoV$_{\Delta ORF6}$=recombinant SARS-CoV with ORF6 knockout mutation.

SARS-CoV or SARS-CoV-2, protein 6 interacts with KPNA1, KPNB1, and Nup93 (SARS-CoV-2 only) and prevents the activation of ISRE promoter elements through STAT1 translocation.[13,14] Our findings complement studies by Miorin and colleagues[14] and Lei and colleagues,[16] showing that charged residues at the CTD of ORF6 can further augment its antagonistic function, probably by increasing interaction with KPNA1 and KPNB1, which has been described to be independent of Nup93 binding via the conserved methionine at amino acid position 58. In summary, these findings show that protein 6 in both viruses is not only genetically homologous, but also functionally homologous.

To our knowledge, this study is the first to use reverse genetics to quantitatively compare protein 6 activity. We found that SARS-CoV-2 protein 6 was less efficient in suppressing interferon signalling than the homologous protein 6 in SARS-CoV. It is relevant to consider this finding in the context of onward evolution of SARS-CoV-2. As the intense circulation of SARS-CoV-2 in the human population might select for more efficient transmissibility, which in turn could be aided by more efficient interferon antagonism, sequence evolution of SARS-CoV ORF6 should be monitored closely. Our mutagenesis study provides a target for sequence-based surveillance, because acquisition of charged amino acids at the CTD of protein 6, specifically at positions Gln51 and Gln56, was found to augment protein 6-dependent interferon signalling suppression in ISRE promotor assays.

Lei and colleagues[16] have described a similar dependency of ISRE promotor activation and charged residue expression in the CTD but did not detect differences in protein 6 activity between the two viruses, which could be caused by reliance on overexpression experiments rather than viral reverse genetics. Nevertheless, both studies together identify a marker for sequence-based surveillance that seems to warrant follow-up studies. It seems relevant that mutants carrying charged residue substitutions at these sites were already detected and have been transmitted. At the same time, many other ORF6 variants were found, often showing stop codon or deletion genotypes that, according to the present results, suggest attenuation. Founder effects, such as those observed with SARS-CoV and SARS-CoV-2 ORF8, seem possible,[32,33] and might contribute to virus attenuation in the long term.

A limitation of this study is that we did not construct further rSARS-CoV variants containing Gln51Glu and Gln56Glu mutations to confirm phenotypic relevance in the context of virus replication. However, natural infection is more complex than infection in cell culture, which is another limitation of the study. Quantitative phenotypic differentiation would thus require the use of more complex models of the human respiratory tract or appropriate animal models.

In conclusion, the present study identifies the gene encoding protein 6 as a genetic marker of virulence that varies between SARS-CoV and SARS-CoV-2, thus providing a target for genome-based surveillance of circulating strains of SARS-CoV-2.

Contributors

SS, MAM, CD, and CG conceived and designed the experiments. SS, FP, and AR did the experiments. SS and DM constructed the recombinant viruses. DN provided material for recombinant virus cloning. TV provided sequence alignments. SS, CD, and MAM interpreted the data. SS and CD wrote the manuscript with input from MAM and CG. SS and CD verified the underlying data. All authors had full access to all the data in the study and SS and CD had final responsibility for the decision to submit for publication.

Declaration of interests

We declare no competing interests.

Data sharing

All imaging raw data haven been deposited on the EMBL-EBI database, under accession number S-BSST525.

Acknowledgments

This work was supported by the Bundesministerium für Bildung und Forschung (grant 01KI1723A), as well as the EU via project RECOVER (GA101003589). Additional funding to CD was provided by Berlin University Alliance, to CG by Berlin Institute of Health, and to CD and CG by OrganoStat (01KX2021).

References

1 Zhu N, Zhang D, Wang W, et al. A novel coronavirus from patients with pneumonia in China, 2019. *N Engl J Med* 2020; **382:** 727–33.
2 Gorbalenya AE, Baker SC, Baric RS, et al. The species severe acute respiratory syndrome-related coronavirus: classifying 2019-nCoV and naming it SARS-CoV-2. *Nat Microbiol* 2020; **5:** 536–44.
3 Wu A, Peng Y, Huang B, et al. Genome composition and divergence of the novel coronavirus (2019-nCoV) originating in China. *Cell Host Microbe* 2020; **27:** 325–28.
4 Hoffmann M, Kleine-Weber H, Schroeder S, et al. SARS-CoV-2 cell entry depends on ACE2 and TMPRSS2 and is blocked by a clinically proven protease inhibitor. *Cell* 2020; **181:** 271–80.e8.
5 Rothe C, Schunk M, Sothmann P, et al. Transmission of 2019-nCoV infection from an asymptomatic contact in Germany. *N Engl J Med* 2020; **382:** 970–71.
6 Wölfel R, Corman VM, Guggemos W, et al. Virological assessment of hospitalized patients with COVID-2019. *Nature* 2020; **581:** 465–69.
7 Bertram S, Heurich A, Lavender H, et al. Influenza and SARS-coronavirus activating proteases TMPRSS2 and HAT are expressed at multiple sites in human respiratory and gastrointestinal tracts. *PLoS One* 2012; **7:** e35876.
8 Wrapp D, Wang N, Corbett KS, et al. Cryo-EM structure of the 2019-nCoV spike in the prefusion conformation. *Science* 2020; **367:** 1260–63.
9 Takaoka A, Yanai H. Interferon signalling network in innate defence. *Cell Microbiol* 2006; **8:** 907–22.
10 Kindler E, Thiel V. To sense or not to sense viral RNA—essentials of coronavirus innate immune evasion. *Curr Opin Microbiol* 2014; **20:** 69–75.
11 Haagmans BL, Kuiken T, Martina BE, et al. Pegylated interferon-alpha protects type 1 pneumocytes against SARS coronavirus infection in macaques. *Nat Med* 2004; **10:** 290–93.
12 Totura AL, Baric RS. SARS coronavirus pathogenesis: host innate immune responses and viral antagonism of interferon. *Curr Opin Virol* 2012; **2:** 264–75.
13 Frieman M, Yount B, Heise M, Kopecky-Bromberg SA, Palese P, Baric RS. Severe acute respiratory syndrome coronavirus ORF6 antagonizes STAT1 function by sequestering nuclear import factors on the rough endoplasmic reticulum/Golgi membrane. *J Virol* 2007; **81:** 9812–24.
14 Miorin L, Kehrer T, Sanchez-Aparicio MT, et al. SARS-CoV-2 Orf6 hijacks Nup98 to block STAT nuclear import and antagonize interferon signaling. *Proc Natl Acad Sci USA* 2020; **117:** 28344–54.
15 Yuen C-K, Lam J-Y, Wong W-M, et al. SARS-CoV-2 nsp13, nsp14, nsp15 and orf6 function as potent interferon antagonists. *Emerg Microbes Infect* 2020; **9:** 1418–28.

16 Lei X, Dong X, Ma R, et al. Activation and evasion of type I interferon responses by SARS-CoV-2. *Nat Commun* 2020; **11:** 3810.

17 Kopecky-Bromberg SA, Martínez-Sobrido L, Frieman M, Baric RA, Palese P. Severe acute respiratory syndrome coronavirus open reading frame (ORF) 3b, ORF 6, and nucleocapsid proteins function as interferon antagonists. *J Virol* 2007; **81:** 548–57.

18 Niemeyer D, Zillinger T, Muth D, et al. Middle East respiratory syndrome coronavirus accessory protein 4a is a type I interferon antagonist. *J Virol* 2013; **87:** 12489–95.

19 Thiel V, Weber F. Interferon and cytokine responses to SARS-coronavirus infection. *Cytokine Growth Factor Rev* 2008; **19:** 121–32.

20 Bertram S, Glowacka I, Blazejewska P, et al. TMPRSS2 and TMPRSS4 facilitate trypsin-independent spread of influenza virus in Caco-2 cells. *J Virol* 2010; **84:** 10016–25.

21 Emanuel W, Kirstin M, Vedran F, et al. Bulk and single-cell gene expression profiling of SARS-CoV-2 infected human cell lines identifies molecular targets for therapeutic intervention. *bioRxiv* 2020; published online May 5. https://doi.org/10.1101/2020.05.05.079194 (preprint).

22 Emeny JM, Morgan MJ. Regulation of the interferon system: evidence that Vero cells have a genetic defect in interferon production. *J Gen Virol* 1979; **43:** 247–52.

23 Yoshikawa T, Hill TE, Yoshikawa N, et al. Dynamic innate immune responses of human bronchial epithelial cells to severe acute respiratory syndrome-associated coronavirus infection. *PloS One* 2010; **5:** e8729.

24 Zielecki F, Weber M, Eickmann M, et al. Human cell tropism and innate immune system interactions of human respiratory coronavirus EMC compared to those of severe acute respiratory syndrome coronavirus. *J Virol* 2013; **87:** 5300–04.

25 Spiegel M, Pichlmair A, Martínez-Sobrido L, et al. Inhibition of beta interferon induction by severe acute respiratory syndrome coronavirus suggests a two-step model for activation of interferon regulatory factor 3. *J Virol* 2005; **79:** 2079–86.

26 Holzinger D, Jorns C, Stertz S, et al. Induction of *MxA* gene expression by influenza A virus requires type I or type III interferon signaling. *J Virol* 2007; **81:** 7776–85.

27 Daffis S, Samuel MA, Keller BC, Gale M Jr, Diamond MS. Cell-specific IRF-3 responses protect against West Nile virus infection by interferon-dependent and -independent mechanisms. *PLoS Pathog* 2007; **3:** e106.

28 Chu H, Chan JF-W, Yuen TT-T, et al. Comparative tropism, replication kinetics, and cell damage profiling of SARS-CoV-2 and SARS-CoV with implications for clinical manifestations, transmissibility, and laboratory studies of COVID-19: an observational study. *Lancet Microbe* 2020; **1:** e14–23.

29 Narayanan K, Huang C, Lokugamage K, et al. Severe acute respiratory syndrome coronavirus nsp1 suppresses host gene expression, including that of type I interferon, in infected cells. *J Virol* 2008; **82:** 4471–79.

30 Niemeyer D, Mösbauer K, Klein EM, et al. The papain-like protease determines a virulence trait that varies among members of the SARS-coronavirus species. *PLoS Pathog* 2018; **14:** e1007296.

31 Devaraj SG, Wang N, Chen Z, et al. Regulation of IRF-3-dependent innate immunity by the papain-like protease domain of the severe acute respiratory syndrome coronavirus. *J Biol Chem* 2007; **282:** 32208–21.

32 Muth D, Corman VM, Roth H, et al. Attenuation of replication by a 29 nucleotide deletion in SARS-coronavirus acquired during the early stages of human-to-human transmission. *Sci Rep* 2018; **8:** 15177.

33 Young BE, Fong S-W, Chan Y-H, et al. Effects of a major deletion in the SARS-CoV-2 genome on the severity of infection and the inflammatory response: an observational cohort study. *Lancet* 2020; **396:** 603–11.